

Inactivation of *Corynebacterium glutamicum* NCgl0452 and the Role of MgtA in the Biosynthesis of a Novel Mannosylated Glycolipid Involved in Lipomannan Biosynthesis*

Received for publication, September 8, 2006, and in revised form, December 1, 2006. Published, JBC Papers in Press, December 19, 2006, DOI 10.1074/jbc.M608695200

Raju V. V. Tatituri^{†1,2}, Petr A. Illarionov^{‡2}, Lynn G. Dover[‡], Jerome Nigou[§], Martine Gilleron[§], Paul Hitchen[¶], Karin Krumbach^{||}, Howard R. Morris^{¶**3}, Neil Spencer^{††}, Anne Dell^{‡,4}, Lothar Eggeling^{||}, and Gurdyal S. Besra^{‡‡5}

From the [†]School of Biosciences, University of Birmingham, Edgbaston, Birmingham B15 2TT, United Kingdom, [§]Institut de Pharmacologie et de Biologie Structurale, UMR CNRS 5089, Toulouse, France, ^{||}Institute for Biotechnology 1, Research Centre Juelich, D-52425 Juelich, Germany, the [¶]Division of Molecular Biosciences, Faculty of Natural Sciences, Imperial College, London SW7 2AZ, United Kingdom, ^{**}M-SCAN Mass Spectrometry Research and Training Centre, Wokingham, Berks RG41 2TZ, United Kingdom, and the ^{††}School of Chemistry, University of Birmingham, Edgbaston, Birmingham B15 2TT, United Kingdom

Mycobacterium tuberculosis PimB has been demonstrated to catalyze the addition of a mannose residue from GDP-mannose to a monoacylated phosphatidyl-*myo*-inositol mannoside (Ac₁PIM₁) to generate Ac₁PIM₂. Herein, we describe the disruption of its probable orthologue Cg-*pimB* and the chemical analysis of glycolipids and lipoglycans isolated from wild type *Corynebacterium glutamicum* and the *C. glutamicum::pimB* mutant. Following a careful analysis, two related glycolipids, Gl-A and Gl-X, were found in the parent strain, but Gl-X was absent from the mutant. The biosynthesis of Gl-X was restored in the mutant by complementation with either Cg-*pimB* or Mt-*pimB*. Subsequent chemical analyses established Gl-X as 1,2-di-O-C₁₆/C_{18:1}-(α -D-mannopyranosyl)-(1 \rightarrow 4)-(α -D-glucopyranosyluronic acid)-(1 \rightarrow 3)-glycerol (ManGlcAGroAc₂) and Gl-A as the precursor, GlcAGroAc₂. In addition, *C. glutamicum::pimB* was still able to produce Ac₁PIM₂, suggesting that Cg-PimB catalyzes the synthesis of ManGlcAGroAc₂ from GlcAGroAc₂. Isolation of lipoglycans from *C. glutamicum* led to the identification of two related lipoglycans. The larger lipoglycan possessed a lipoarabinomannan-like structure, whereas the smaller lipoglycan was similar to lipomannan (LM). The absence of ManGlcAGroAc₂ in *C. glutamicum::pimB* led to a severe reduction in LM. These results suggested that ManGlcAGroAc₂ was further extended to an LM-like molecule. Complementation of *C. glutamicum::pimB* with Cg-*pimB* and Mt-*pimB* led to the restoration of LM biosynthesis. As a result, Cg-PimB, which we have assigned as MgtA, is now clearly defined as a GDP-mannose-dependent α -mannosyltransferase from our *in vitro* analyses and is involved in the biosynthesis of ManGlcAGroAc₂.

The *Corynebacteriaceae* represent a distinct and unusual group within Gram-positive bacteria, with the most prominent members being the human pathogens *Mycobacterium tuberculosis* and *Mycobacterium leprae* (1). In addition, the human pathogen *Corynebacterium diphtheriae* is the causal agent of diphtheria, and serious economic losses occur from the infection of animals by corynebacteria, such as *Corynebacterium pseudotuberculosis* and *Corynebacterium matruchotii* (2, 3). Furthermore, nonpathogenic bacteria belong to this taxon, such as *Corynebacterium glutamicum*, which is used in the industrial production of amino acids (4, 5).

A common feature to all these bacteria is that they possess an unusual cell wall matrix composed of mycolic acids, arabinogalactan, and peptidoglycan that is often referred to as the mycolyl-arabinogalactan-peptidoglycan complex (6–13). In addition, they also possess a similar array of cell wall-associated glycolipids, such as phosphatidyl-*myo*-inositol (PI)⁶ mannosides (PIMs) and lipoglycans, termed lipomannan (LM) and lipoarabinomannan (LAM) (12, 14–18).

Four major PIMs, mono- and diacyl dimannosides (Ac₁PIM₂ and Ac₂PIM₂) and mono- and diacyl hexamannosides (Ac₁PIM₆ and Ac₂PIM₆), usually accumulate (12) with intermediates occurring in low abundance. Furthermore, the characteristic mycobacterial lipoglycans, LAM and LM, are both multiglycosylated versions of PIMs. We initially proposed the biosynthetic pathway PI \rightarrow PIM \rightarrow LM \rightarrow LAM (15), which is now largely supported by biochemical and genetic evidence (19–22). PimA catalyzes the addition of Manp provided by GDP-mannose to the 2-position of the *myo*-inositol of PI to form PIM₁ (21), whereas PimB might be responsible for the addition of a second Manp to the 6-position to yield Ac₁PIM₂

* The costs of publication of this article were defrayed in part by the payment of page charges. This article must therefore be hereby marked "advertisement" in accordance with 18 U.S.C. Section 1734 solely to indicate this fact.

¹ A Darwin Trust-sponsored Ph.D. student.

² These authors contributed equally to this work.

³ Supported by funding from the Biotechnology and Biological Sciences Research Council and the Wellcome Trust.

⁴ A Biotechnology and Biological Sciences Research Council Professorial Research Fellow.

⁵ Supported by a Personal Research Chair from James Bardrick, as a former Lister Institute-Jenner Research Fellow, the Medical Research Council and The Wellcome Trust. To whom correspondence should be addressed. Tel.: 121-415-8125; Fax: 121-414-5925; E-mail: g.besra@bham.ac.uk.

⁶ The abbreviations used are: PI, phosphatidyl-*myo*-inositol; Ac, acyl; Ara, arabinose; CID, collision-induced dissociation; Cg, *C. glutamicum*; f, furanose; GC, gas chromatography; MS, mass spectrometry; GlcA, glucopyranosyluronic acid; Gro, glycerol; p, pyranose; MALDI, matrix-assisted laser desorption/ionization; TOF, time of flight; Mt, *M. tuberculosis*; PIM, phosphatidyl-*myo*-inositol mannosides; LM, lipomannan; LAM, lipoarabinomannan; ManGlcAGroAc₂, 1,2-di-O-C₁₆/C_{18:1}-(α -D-mannopyranosyl)-(1 \rightarrow 4)-(α -D-glucopyranosyluronic acid)-(1 \rightarrow 3)-glycerol; MOPS, 4-morpholinepropanesulfonic acid; NOE, nuclear Overhauser effect; NOESY, NOE spectroscopy; HOHAHA, homonuclear Hartman Hahn.

TABLE 1

Strains and plasmids used in this study

| | Relevant characteristics | Source |
|----------------------------------|--|-----------|
| Strains | | |
| <i>E. coli</i> DH5 α mc | F- <i>endA1 supE44 thi-1 λ-recA1 gyrA96 relA1 deoR Δ(lacZYA-argF)</i> | Ref. 26 |
| <i>C. glutamicum</i> 13032::pimB | Wild type ATCC13032 | ATCC |
| 13032::pimB pEKEx3 | Wild type with Cg-pimB inactivated | This work |
| 13032::pimB pEKEx3-Cg-pimB | Inactivation mutant with control plasmid | This work |
| 13032::pimB pEKEx3-Mt-pimB | Inactivation mutant with Cg-pimB overexpressed | This work |
| | Inactivation mutant with Mt-pimB overexpressed | This work |
| Plasmids | | |
| pK19mobsacB | Integration vector, Km ^r <i>oriV_{Ec}</i> <i>oriT</i> <i>sacB</i> | Ref. 27 |
| pK19mobsacB::pimB | Vector for inactivation of Cg-pimB | This work |
| pEKEx3 | Expression vector, Spec ^r | Ref. 28 |
| pEKEx3-Cg-pimB | Vector for overexpression of Cg-pimB | This work |
| pEKEx3-Mt-pimB | Vector for overexpression of Mt-pimB | This work |

(19). PimC has been demonstrated to allow further mannosylation to Ac₁PIM₃ (20), and more recently PimE has been shown to be involved in the biosynthesis of Ac₁PIM₅ (23). It has been proposed that PIM₄ is the direct precursor of LM, characterized by a linear α (1 \rightarrow 6)-linked mannan backbone linked with α (1 \rightarrow 2) mannopyranose side chains generated through Rv2181 (24). LM is then further glycosylated with arabinan to produce LAM and finally “mannose-capped” to produce ManLAM, a process initiated by the capping enzyme encoded by Rv1635c (25).

In the present study, we have established that *C. glutamicum* possesses both PIMs and lipoglycans, which are reminiscent of *M. tuberculosis* products, suggesting that conserved biosynthetic machineries are present within these two bacteria. Interestingly, the polar lipid profile revealed a previously uncharacterized major glycolipid. Furthermore, disruption of *pimB* in *C. glutamicum* abolished the synthesis of this novel glycolipid, which had a subsequent profound effect on LM biosynthesis. In addition, complementation with either Cg-pimB or Mt-pimB led to the restoration of wild type glycolipid and lipoglycan biosynthesis.

EXPERIMENTAL PROCEDURES

Strains and Culture Conditions—The strains and plasmids used are given in Table 1 (26–28). *C. glutamicum* ATCC 13032 (wild type) and *Escherichia coli* DH5 α mc were grown in Luria-Bertani broth (LB; Difco) at 30 and 37 °C, respectively. For *C. glutamicum*, kanamycin was used at a concentration of 25 μ g/ml, and spectinomycin was used at a concentration of 250 μ g/ml where appropriate. The minimal medium used for *C. glutamicum* was CGXII, and mutants were selected on LBHIS (28). Samples for lipid analyses were prepared by harvesting cells grown either on BHIS for 9 h up to an $A_{600\text{ nm}}$ of 7–8 or on CGXII for 17 h up to $A_{600\text{ nm}}$ of 47–51. Cells were harvested by centrifugation, followed by saline washing and freeze drying. *M. tuberculosis* H37Rv DNA was obtained from Dr. J. T. Belisle and the NIH Tuberculosis Research Materials and Vaccine Testing Contract at Colorado State University. All other chemicals were reagent grade or better and obtained from Sigma.

Construction of Plasmids—The inactivation vector pK19mobsacB::pimB was made by amplification of a 359-bp internal fragment of *C. glutamicum* *pimB* using the primer pair p557up and p557low (Table 2). After purification and treatment with polynucleotide kinase, the fragment was ligated with

TABLE 2

PCR primers

Restriction enzyme recognition sites are in boldface type, and the ribosome binding site is in italic type.

| Name | Primer |
|------------|--|
| p557up | 5'-TTGGCCACTGCAAGCTGGGAAT-3' |
| p557low | 5'-TGTGAAGATCGCATCCGGCATC-3' |
| p557up2 | 5'-TGATGTCGACGGTTCTCCAG-3' |
| p557low2 | 5'-GTTGATCAAAATCAATGGGACCACC-3' |
| puni | 5'-CGCCAGGGTTTTCACAGTCACGAC-3' |
| prsp1 | 5'-CACAGGAAACAGCTATGACCATG-3' |
| p557up3 | 5'-CGC AGTACT AAGGAGATATAGATGTGGAGATAAT AAGGCCATG-3' |
| p557low3 | 5'-CGC GAATTC TTAAGCCTCGATGCTGATGCGG-3' |
| ppimBMtex | 5'-TCC CCCGGG AAGGAGATATAGATGTGTGTGGCGT GCGCGTTGC-3' |
| ppimBMtrev | 5'-CGGAATTCCTACGCGCCTGGGTCTGTC-3' |

SmaI-cleaved pK19mobsacB. To construct pEKEx3-Cg-pimB, chromosomal DNA of *C. glutamicum* together with primers p557up3 and p557low3 and KOD DNA polymerase were used to amplify Cg-pimB. The resulting 1232-bp fragment was cloned into the SmaI site of pUC18, from which the fragment was reisolated by digestion with ScaI/EcoRI to ligate it with SmaI/EcoRI-cleaved pEKEx3. Similarly, Mt-pimB was amplified using primers ppimBMtex and ppimBMtrev using *M. tuberculosis* chromosomal DNA. The resulting 1153-bp fragment was cloned into pUC18, subsequently excised as a SmaI/EcoRI fragment, which was ligated with SmaI/EcoRI-cleaved pEKEx3. All cloned fragments were verified by nucleotide sequencing.

Construction of Strains—Cells of *C. glutamicum* were made competent as described (28) and transformed by electroporation with pK19mobsacB::pimB to kanamycin resistance, signifying the integration of the construct into the chromosome. Using the two different primer pairs prsp1/p557up2 and puni/p557low2, respectively, the correct disruption of Cg-pimB integration was verified. Competent cells of one disruption mutant were chosen and transformed by electroporation with either pEKEx3-Cg-pimB or pEKEx3-Mt-pimB to spectinomycin resistance, and the plasmid integrity of the recombinant clones was confirmed in plasmid preparations.

Lipid Extraction and Analysis—Polar lipids and apolar lipids were initially extracted from 6 g of dry *C. glutamicum* cells according to the procedures of Dobson *et al.* (29) by stirring in 220 ml of methanolic saline (20 ml of 0.3% NaCl and 200 ml of CH₃OH) and 220 ml of petroleum ether for 2 h. The cells were centrifuged at 3000 rpm for 5 min. The resulting biphasic solu-

tion was separated, and the upper layer containing apolar lipids was recovered. An additional 220 ml of petroleum ether was added, mixed, and harvested as described above. The two upper petroleum ether fractions were combined and dried under reduced pressure.

To extract polar lipids, 260 ml of CHCl_3 , CH_3OH , 0.3% NaCl (9:10:3, v/v/v) was added to the lower aqueous CH_3OH layer, and the solution was stirred for 4 h. This mixture was filtered, and the filter cake was re-extracted twice with 85 ml of CHCl_3 , CH_3OH , 0.3% NaCl (5:10:4, v/v/v). CHCl_3 (145 ml) and 0.3% NaCl (145 ml) were added to the combined filtrates. This mixture was stirred for 1 h and allowed to settle, and the lower layer containing the polar lipids was recovered and dried under reduced pressure. The polar lipid extract was examined by two-dimensional TLC on aluminum-backed plates of silica gel 60 F₂₅₄ (Merck 5554), using CHCl_3 , CH_3OH , H_2O (65:25:4, v/v/v) in the first direction and CHCl_3 / CH_3COOH / CH_3OH / H_2O (40:25:3:6, v/v/v/v) in the second direction (29). Glycolipids were visualized by spraying plates with α -naphthol/sulfuric acid followed by gentle charring of plates, by spraying with 5% ethanolic molybdophosphoric acid and charring, or by using a Dittmer and Lester reagent that is specific for phospholipids and glycolipids.

Purification of Glycolipids—The crude polar lipid extract (250 mg) was dissolved in CHCl_3 / CH_3OH (2:1, v/v) and applied to a DEAE-cellulose column (2 × 15 cm) for purification. The column was eluted with CHCl_3 / CH_3OH (100 ml; 2:1, v/v) and increasing concentrations of ammonium acetate (1–500 mM) in CHCl_3 / CH_3OH (2:1, v/v). The purification process was monitored by TLC using either CHCl_3 / CH_3OH / H_2O (65:25:4, v/v/v) or CHCl_3 / CH_3COOH / CH_3OH / H_2O (40:25:3:6, v/v/v/v) (29). Glycolipids were visualized by spraying plates with α -naphthol/sulfuric acid followed by gentle charring of the plates. Lipid phosphates were stained and visualized using a modification of the Dittmer-Lester reagent for TLC (30). Glycolipids were further purified into individual species by preparative TLC on 10 × 20-cm plastic-backed TLC plates of silica gel 60 F₂₅₄ (catalog number 5735; Merck), run in CHCl_3 / CH_3OH / H_2O (65:25:4, v/v/v). The plates were sprayed with 0.01% 1,6-diphenyl-1,3,5-hexatriene dissolved in petroleum ether/acetone (9:1, v/v), and the glycolipids were visualized under UV light. Following detection, the plates were redeveloped in toluene, and the corresponding purified glycolipid bands were scraped from the plates and extracted from the silica gel using CHCl_3 / CH_3OH (2:1, v/v).

In Vitro Synthesis of Radiolabeled Mannolipids—*C. glutamicum* strains ATCC 13032 and the 13032::pimB mutant transformed with either pEKEx3, pEKEx3-Gg-pimB, or pEKEx3-Mt-pimB were cultured to the midlogarithmic growth phase in 2 liters of BHIS medium with appropriate antibiotics. Cells were harvested by centrifugation; resuspended in 20 ml of 50 mM MOPS, pH 7.9, 5 mM 2-mercaptoethanol, 5 mM MgCl_2 ; and lysed immediately by passing twice through a French pressure cell (aperture pressure change = 3000 p.s.i.). The lysate was clarified by centrifugation at 27,000 × g (4 °C, 30 min), and membranes were deposited by centrifugation of the supernatant at 105,000 × g (4 °C, 90 min). The membrane pellet was gently resuspended in the above buffer to 250 μl and supple-

mented with CaCl_2 to 10 mM and 25 μg of amphomycin in order to inhibit transfers of radiolabel to polyprenyl phosphate acceptors. This mixture was held at 37 °C for 15 min prior to the addition of 0.25 μCi of GDP-Man (0.3054 Ci/mmol; GE Healthcare). The reaction was held at 37 °C for a further 45 min before quenching with 4 ml of CHCl_3 / CH_3OH / H_2O (10:10:3, v/v/v). A biphasic was formed by the addition of 1.75 ml of CHCl_3 and 0.55 ml of H_2O . The lower organic phase was washed twice with 2 ml of CHCl_3 / CH_3OH / H_2O (3:47:48, v/v/v). The extract was dried, and radioactivity was quantified by liquid scintillation counting of a sample of the extract. Two-dimensional TLC analysis was carried out as above, and the mannolipids formed were visualized by phosphorimaging (Kodak K Screen).

Extraction and Purification of Lipoglycans—Lipoglycans were extracted from delipidated cells as previously described (31, 32). Briefly, cells were broken by sonication (MSE Soniprep 150; 12- μm amplitude, 60 s on, 90 s off for 10 cycles, on ice) and the cell debris was refluxed five times with 50% $\text{C}_2\text{H}_5\text{OH}$ at 68 °C for 12-h intervals. The cell debris was removed by centrifugation, and the supernatant containing lipoglycans, neutral glycans, and proteins dried. This dried extract was then treated with hot phenol- H_2O . The aqueous phase was dialyzed and dried before separate and extensive treatments with α -amylase, DNase, and RNase chymotrypsin and trypsin. Finally, the lipoglycan fraction was dialyzed extensively against water.

The crude lipoglycan extract was resuspended in buffer A (50 mM ammonium acetate and 15% propan-1-ol) and subjected to octyl-Sepharose CL-4B hydrophobic interaction chromatography (2.5 × 50 cm) as previously reported (33). The column was initially washed with 4 column volumes of buffer A to ensure removal of neutral glycans, followed by buffer B (50 mM ammonium acetate and 50% propan-1-ol). The eluate was collected and concentrated to ~1 ml and precipitated using 5 ml of $\text{C}_2\text{H}_5\text{OH}$, and the sample was dried using a Savant SpeedVac. The freeze-dried sample containing the retained material from the hydrophobic interaction column was then resuspended in buffer C (0.2 M NaCl, 0.25% sodium deoxycholate (w/v), 1 mM EDTA, and 10 mM Tris-HCl, pH 8) to a final concentration of 200 mg/ml. The sample was gently mixed and left to incubate for 48 h at room temperature. The sample was then loaded onto a 200 ml Sephacryl S-200 column previously equilibrated with buffer C. The sample was eluted with 400 ml of buffer C at a flow rate of 3 ml/h, collecting 1.5-ml fractions. The fractions were monitored by SDS-PAGE using either a silver stain utilizing periodic acid and silver nitrate (34) or a Pro-Q emerald glycoprotein stain (Invitrogen), and individual fractions were pooled and dialyzed extensively against buffer D (10 mM Tris-HCl, pH 8, 0.2 M NaCl, 1 mM EDTA) for 72 h with frequent changes of buffer. The samples were further dialyzed against deionized water for 48 h with frequent changes of water, lyophilized, and stored at –20 °C.

Glycosyl Compositional and Linkage Analysis—Glycosyl compositional analysis was performed by either routine gas chromatography (GC) or capillary electrophoresis analysis as described previously (35). Glycosyl linkage analyses were performed as described previously (36). Briefly, per-O-methylated samples were hydrolyzed using 500 μl of 2 M trifluoroacetic acid

Identification of a Novel Mannosylated Glycolipid

at 110 °C for 2 h, reduced using 350 μ l of a 10 mg/ml solution of NaBD₄ (1 M aqueous NH₄OH/C₂H₅OH, 1:1, v/v), and per-*O*-acetylated using 300 μ l of acetic anhydride for 1 h at 110 °C. The resulting alditol acetates were solubilized in cyclohexane before analysis by GC and gas chromatography/mass spectrometry (GC/MS) (37).

GC analysis was performed using a Thermoquest Trace GC 2000 equipped with a flame ionization detector. Samples were separated using a temperature program as follows. Injector temperature was set at 50 °C, held for 1 min, and then increased to 110 °C at 20 °C/min. The oven was held at 110 °C and then ramped to 290 °C at 8 °C/min and held for 5 min to ensure that all of the products had eluted from the column. All of the data were collected and analyzed using Xcaliber (version 1.2) software.

Gl-A, Gl-X, and Ac₁PIM₂ Matrix-assisted Laser Desorption Ionization-Time of Flight-Mass Spectrometry (MALDI-TOF-MS) Analyses—Analyses of PIMs were carried out on a Voyager DE-STR MALDI-TOF instrument (PerSeptive Biosystems, Framingham, MA) using the reflectron mode of detection as previously described (38). PIMs were analyzed by the instrument operating at 20 kV in the negative ion mode, using an extraction delay time set at 200 ns. Typically, spectra from 100–250 laser shots were summed to obtain the final spectrum. All of the samples were prepared for MALDI-TOF-MS analyses using the on-probe sample clean-up procedure with cation exchange resin. The 2-(4-hydroxyphenylazo)-benzoic acid matrix was used at a concentration of 10 mg/ml in C₂H₅OH/H₂O (1:1, v/v). Typically, 0.5 μ l of PIM sample (10 μ g) in a CHCl₃/CH₃OH/H₂O solution and 0.5 μ l of the matrix solution, containing 5–10 cation exchange beads, were deposited on the target, mixed with a micropipette, and dried under a gentle stream of warm air.

Analyses of the Gl-A and Gl-X were carried out on a 4700 Proteomics Analyzer (with TOF-TOF optics; Voyager DE-STR; Applied Biosystems, Framingham, MA) using the reflectron mode. Ionization was effected by irradiation with a Nd:YAG laser (355 nm) operating by pulses of 500 ps with a frequency of 200 Hz. Gl-A and Gl-X were analyzed in the positive ion mode. Spectra from 2500 to 5000 laser shots were summed to obtain the final spectrum. Typically, 0.3 μ l of Gl-X (at 10 mg/ml in CHCl₃/CH₃OH, 1:1, v/v) and 0.3 μ l of the matrix solution (2,5-dihydrobenzoic acid at ~10 mg/ml in C₂H₅OH/H₂O, 1:1, v/v) were deposited on the target. Collision-induced dissociation (CID)-MS/MS was performed using atmosphere as the gas type. The pressure was set to medium, and the collision energy was set to 1 kV.

Analysis of per-*O*-methylated Gl-X was performed using an Applied Biosystems 4800 MALDI-TOF/TOF in the positive mode. MS/MS was performed with the collision energy set to 1 kV with air as the collision gas. The per-*O*-methylated sample was dissolved in CH₃OH, and 0.5- μ l aliquots were loaded onto the target plate with 0.5 μ l of the matrix 2,5-dihydrobenzoic acid at 10 mg/ml in CH₃OH/H₂O. Sequazyme peptide mass standards were used as external calibrants (Applied Biosystems).

NMR Spectroscopy—NMR spectra of lipoglycans were recorded on a Bruker DMX-500 equipped, with a double reso-

nance (¹H/¹³C)-BBI z-gradient probe head. All samples were exchanged in D₂O (D, 99.97% from Euriso-top, Saint-Aubin, France), with intermediate lyophilization, and then dissolved in 0.5 ml of D₂O and analyzed at 313 K. The ¹H and ¹³C NMR chemical shifts were referenced relative to internal acetone at 2.225 and 34.00 ppm, respectively. All of the details concerning NMR sequences used and experimental procedures were described in previous studies (39, 40).

Gl-X NMR spectra were recorded in *d*₆-Me₂SO. NMR spectra were recorded on a Bruker DRX500 operating at 500.13 MHz for ¹H and 125.77 MHz for ¹³C. The instrument was equipped with a 5-mm ¹H-¹³C-{X}-triple broadband inverse triple resonance z-gradient probe head, and all spectra were run at 300 K. *d*₆-Me₂SO was used as lock, and the residual solvent was used as internal reference (2.49 ppm for ¹H and 39.5 ppm for ¹³C). Data were acquired and processed using XWINNMR version 2.6 software on a Silicon Graphics work station. The ¹³C NMR data were acquired with ¹H decoupling and NOE. Additionally and under the same conditions, a DEPT-135 experiment was performed to provide spectral editing information. All two-dimensional NMR data were acquired nonspinning. Data points (2048) were used in acquisition for the fast domain (F2), and 512 points were used in the incremented domain (F1). The F1 dimension was zero-filled to 1024 data points in processing. The gradient COSY-90 data were transformed using a magnitude calculation, and a nonshifted sine bell window function was used in both frequency domains. The HSQC, NOESY, and T-ROESY NMR experiments (all performed using pulsed field gradients) were acquired in phase-sensitive mode using the time-proportional phase increment for the HSQC and NOESY experiments, whereas the States-time-proportional phase increment was used for the T-ROESY experiment. In all three experiments, a Qsine window function shifted by $\pi/2$ was used for both frequency domains in processing. GARP decoupling was employed in F1 for the HSQC experiment. A mixing period of 450 ms was employed in the NOESY experiment. A mixing period of 400 ms was used in the T-ROESY experiment. To minimize the HOHAHA contribution to the T-ROESY data, a spin lock field of 8.8 kHz was used, and the transmitter was offset by 8.8 kHz (during the spin lock period only). The spin lock field was also ramped using a Squar-ramp20 shaped pulse (described by 1000 points). In both NOESY and T-ROESY experiments, 24 transients/increment were employed.

RESULTS

Genomic Organization of the pimB Locus—Mt-*pimB* has been shown to encode an α -mannosyltransferase potentially involved in Ac₁PIM₂ biosynthesis (19), and this gene is predicted to be essential in *M. tuberculosis* (41). However, the biosynthesis of PIMs remain unaffected upon disruption of Mt-*pimB*,⁷ suggesting either a degree of redundancy or that Mt-*pimB* performed another function in *M. tuberculosis*. Mt-*pimB* lies within a cluster of genes involved in menaquinone biosynthesis (Fig. 1A). Directly upstream is a small open reading frame of unknown function and *menD*, and directly down-

⁷ G. S. Besra and L. S. Schlesinger, unpublished data.

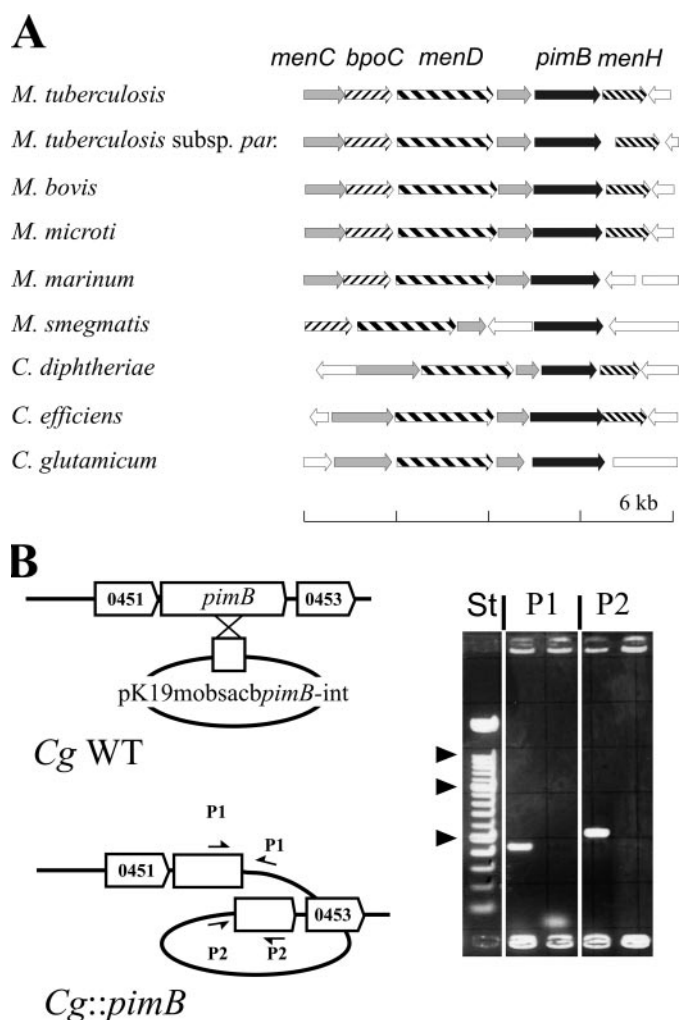


FIGURE 1. Comparison of the *pimB* locus within the *Corynebacteriaceae* and inactivation of *Cg-pimB*. A, the locus consists in *M. tuberculosis* of *Mt-pimB* with adjacent genes presumably involved in the biosynthesis of menaquinone and a bromoperoxidase (*bpoC*). The locus in other *Mycobacterium* species and *Corynebacterium* species is largely syntenic. *par.*, *paratuberculosis*. B, construction of *C. glutamicum* 13032::*pimB*. Shown is *Cg-pimB* with its adjacent genes NCgl0451 and NCgl0453 and the strategy to disrupt *Cg-pimB* using vector pK19mobsacBpimB-int. This vector carries a 359-bp internal fragment of *Cg-pimB* of 1221 bp in size, thereby enabling homologous recombination with the wild type genome to generate *C. glutamicum*::*pimB*. The arrow pairs marked P1 (prsp1/p557up2) and P2 (puni/p557low2) locate the primers used for the PCR analysis to confirm the proper integration of vector pK19mobsacBpimB-int in *C. glutamicum* 13032::*pimB* and its absence in wild type *C. glutamicum*. The results of the PCR analysis are shown on the right, where P1 and P2 mark the result obtained with primers P1 and P2, respectively. Samples were applied pairwise with the amplificate obtained from *C. glutamicum* 13032::*pimB* applied in the left lane, exhibiting the expected PCR products of 442 and 603 bp, respectively, whereas these were absent in wild type *C. glutamicum* (WT). St marks the standard, and the arrowheads are located at 0.5, 1, and 1.5 kb, respectively.

stream is *menH*. The entire locus consisting of seven genes is syntenic in all sequenced *Mycobacterium* species and, in part, also in *Corynebacterium*, both genera belonging to the taxon *Corynebacteriaceae* (Fig. 1A). The putative orthologue of *Mt-pimB* from *C. glutamicum*, *Cg-pimB* (NCgl0452), shares 49% sequence identity with the *M. tuberculosis* gene, and, since *C. glutamicum* can be regarded as a model organism of this taxon due to its archetypical genomic organization as manifested in a low number of gene duplications, its structural simplicity, and

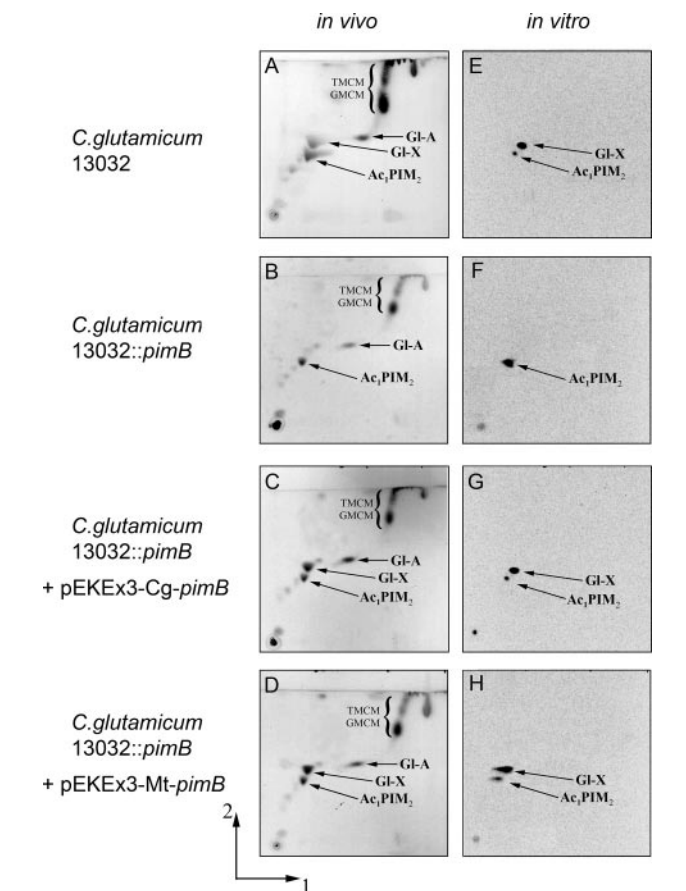


FIGURE 2. In vivo and in vitro analyses of *C. glutamicum* glycolipid biosynthesis. The polar lipid profiles of wild type *C. glutamicum* (A and E), the *C. glutamicum* 13032::*pimB* disruption mutant (B and F), and the *C. glutamicum* 13032::*pimB* mutant complemented with *Cg-pimB* (C and G) and *Mt-pimB* (D and H), respectively, are shown. The polar lipid extract was examined by two-dimensional thin layer chromatography on aluminum-backed plates of silica gel 60 F₂₅₄ (Merck 5554), using CHCl₃/CH₂OH/H₂O (65:25:4, v/v/v) in the first direction and CHCl₃/CH₂COOH/CH₂OH/H₂O (40:25:3:6, v/v/v) in the second direction (29). Glycolipids were visualized by spraying plates with α -naphthol/sulfuric acid, followed by gentle charring of the plates (A–D). E–H show *in vitro* labeling of polar lipids utilizing GDP-[¹⁴C]Man, and products were analyzed using the same two-dimensional TLC system. The novel glycolipids GL-X and GL-A, and Ac₁PIM₂ are highlighted.

ease of handling (42), we decided to study the function of *Mt-pimB* in more detail using *C. glutamicum*.

Construction and Growth of the *C. glutamicum* 13032::*pimB* Disruption Mutant—*C. glutamicum* ATCC13032 was transformed to kanamycin resistance with plasmid pK19mobsacB::*pimB* (Fig. 1B) using the method we have previously reported (43, 44). Fourteen colonies were obtained from 1 μ g of plasmid DNA. The clones were analyzed via PCR, and all were found to have the vector integrated chromosomally, thus demonstrating disruption of the *Cg-pimB* coding sequence. One strain was chosen and termed 13032::*pimB*. This strain displayed no detectable change in phenotype in terms of growth rate or colony morphology (data not shown) and was transformed with either pEKEx3-*Cg-pimB* or pEKEx3-*Mt-pimB* as well as the unmodified vector, pEKEx3, as a control for further studies.

Chromatographic Analysis of Polar Lipids—Polar lipids were extracted from wild type *C. glutamicum*, and glycolipid profiles were recorded by two-dimensional TLC (Fig. 2). The faster

migrating lipids were confirmed as trehalose monocorynomycolate and glucose monocorynomycolate (data not shown). Interestingly, in the pattern shown in Fig. 2A, not all of the remaining glycolipids gave a positive response with the Dittmer-Lester lipid phosphate reagent. The predominant lipid phosphate spot, which was also carbohydrate-positive, corresponded to Ac_1PIM_2 and was confirmed by negative ion mode MALDI-MS analyses due to the characteristic ions at m/z 1398 ($\text{M} - \text{H}$)[−] and in positive mode at m/z 1444 ($\text{M} - \text{H} + 2\text{Na}$)⁺ (data not shown). The phosphorus-free glycolipid, indicated as Gl-X (Fig. 2A) was unusual in terms of chromatographic mobility and staining properties. Analysis of the *C. glutamicum* 13032::pimB disruption mutant revealed that synthesis of Ac_1PIM_2 was intact; however, it failed to produce Gl-X (Fig. 2B). Transformation with pEKEx3-Cg-pimB complemented the mutant phenotype and restored Gl-X biosynthesis (Fig. 2C). Transformation with pEKEx3-Mt-pimB also restored the wild type phenotype, suggesting that the product of Mt-pimB was able to complement the lesion in Gl-X biosynthesis in the mutant (Fig. 2D).

To further clarify the structure of Gl-X and the role of Cg-pimB, the crude polar lipid extract was fractionated using anion exchange chromatography on DEAE-cellulose using a stepwise gradient of increasing ammonium acetate concentration in $\text{CHCl}_3/\text{CH}_3\text{OH}$ ranging from 1 mM to 500 mM. It was anticipated that since Gl-X was phosphorus-negative, this would provide a convenient purification protocol allowing the neutral glycolipid to elute from the column while retaining the contaminating phospholipids. Surprisingly, Gl-X was also retained on the DEAE column and was eluted with 15 mM ammonium acetate in $\text{CHCl}_3/\text{CH}_3\text{OH}$ (2:1), just before Ac_1PIM_2 , suggesting that it possesses an acidic group. Pooled fractions containing Gl-X were pooled, and the lipid was purified further by preparative TLC and analyzed by MALDI-TOF-MS, ^1H , ^{13}C two-dimensional COSY, and two-dimensional HSQC NMR.

Chemical Composition of Gl-X—Initial glycosyl compositional analysis using alditol acetates determined the presence of mannose by GC (data not shown). ^1H and ^{13}C NMR spectra recorded in d_6 -Me₂SO were in agreement with a diglycosyl diacylated glycerol. Indeed, the ^1H - ^{13}C HSQC NMR spectrum showed two anomeric resonances at $\delta_{\text{H1/C1}}$ 4.98/100.3 (I_1) and 4.57/99.0 (II_1). The diacylated glycerol unit was identified by two-dimensional ^1H - ^1H COSY NMR spectrum (Fig. 3A) from its deshielded H-2 (III_2) proton resonance at 5.09 ppm that correlated with H-1, H-1', H-3, and H3' resonances at 4.15 (III_1), 4.31 (III_1'), 3.45 (III_3), and 3.65 (III_3') ppm, respectively. Glycerol carbons resonated at 62.2 (C-1), 69.4 (C-2), and 64.8 (C-3) ppm in agreement with the literature (39).

Gl-X was subsequently analyzed both in negative and positive mode MALDI-TOF-MS. Spectra were only obtained in positive mode, revealing a molecular ion at m/z 977 (Fig. 4A). Positive ion MALDI-TOF CID-MS/MS spectrum of the cationized sodiated precursor ion ($\text{M} - \text{H} + 2\text{Na}$)⁺ of Gl-X revealed ions at m/z 721 and 695, corresponding to the loss of C_{16} and $\text{C}_{18:1}$ fatty acids, respectively (Fig. 4B), which were also later confirmed by fatty acid methyl ester analysis by GC/MS (data not shown).

However, a simple Man-Man-GroAc₂ (containing no inositol) and both mannose units interconnected did not coincide with the deduced molecular weight (m/z 977), suggesting that we were not dealing with a simple Man-Man type structure but a Man-Y-GroAc₂ with Y possibly carrying an acidic function, explaining the retention of Gl-X on DEAE-cellulose. Indeed, the molecular ion at m/z 977 is in agreement with a Man-Y-Gro- $\text{C}_{16}/\text{C}_{18:1}$ structure, where Y represents a hexosyl uronic acid in the ($\text{M} - \text{H} + 2\text{Na}$)⁺ form. MALDI-TOF/TOF analysis of the per-O-methylated Gl-X glycan observed at m/z 579 ($\text{M} + \text{Na}$)⁺ gave data rich in informative fragment ions (Fig. 4C). In particular, the data are indicative of Y being consistent with a hexuronic acid (Fig. 4C, inset). These assignments were substantiated by MS/MS analysis of the per-O-deuteriomethylated glycan observed at m/z 606 ($\text{M} + \text{Na}$)⁺. Furthermore, mild hydrolysis of the per-O-deuteriomethylated glycan with methanolic HCl resulted in a shift of 3 mass units to m/z 603, consistent with methyl exchange on the carboxylic group of hexuronic acid.

The linkage of the two different glycosyl units was established from ^1H - ^1H ROESY, T-ROESY NMR, and ^{13}C NMR experiments (data not shown) that revealed that C-4 of the unit II at 78.6 ppm was shifted to low field away from the remaining resonances at 68–74 ppm. H-1 of unit I (I_1) at 4.98 ppm showed an intense interresidue NOE with H-4 of unit II (II_4) at 3.59 ppm and weaker NOE with H-5 (II_5) and H-3 (II_3) of unit II at 3.53 and 3.48 ppm, respectively. Taken together, these data indicate that unit I is linked at O-4 of unit II. ^1H and ^{13}C resonances of spin system I correlate with a t-Man_p unit, with an α -anomeric configuration suggested by the presence of an intense intrasidue contact between H-1 at 4.98 ppm (I_1) and H-2 at 3.64 ppm (I_2) and the absence of an intrasidue H-1/H-3 NOE contact.

Based on the assignment of ^1H - ^1H COSY NMR and proton coupling constants, unit II (sugar Y) was shown to be α -D-glucopyranosyluronic acid as follows. The small $J_{1,2}$ coupling constant (3.2 Hz) of H-1 at 4.57 ppm (II_1) indicated an α -anomeric configuration. The large coupling constant of H-2 (dd) at 3.19 ppm (II_2) $J_{2,3}$ (9.6 Hz), H-4 (t) at 3.59 ppm (II_4) $J_{3,4}$ (9.6 Hz), H-5 (d) at 3.53 ppm (II_5) $J_{4,5}$ (9.6 Hz) correlates with a *gluco*-configuration of sugar Y. The connectivity of H-5 (II_5) to only one proton H-4 (II_4) in the two-dimensional COSY NMR spectra while a distinct signal for an extra carboxyl group at 171.6 in the ^{13}C NMR spectra is clearly visible indicating that sugar Y is uronic acid. In addition, H-1 of glucuronic acid (II_2) at 4.57 ppm showed an interresidue NOE contact with H-3 of the glycerol unit (III_3) at 3.45 ppm, demonstrating that unit II is linked at O-3 of the glycerol backbone. The complete assignment of resonances of both glycosyl residues is given in Table 3.

Altogether, these data indicate a 1,2-di-O- $\text{C}_{16}/\text{C}_{18:1}$ -(α -D-mannopyranosyl)-(1→4)-(α -D-glucopyranosyluronic acid)-(1→3)-glycerol structure. In addition, and due to the significant sequence identity (49%) between Cg-PimB and Mt-PimB and their similarity to other GDP-mannose-dependent α -mannosyltransferases, it is now persuasive to argue that PimB is involved in the biosynthesis of Gl-X, which we have solved as ManGlcAGroAc₂ (Fig. 3B).

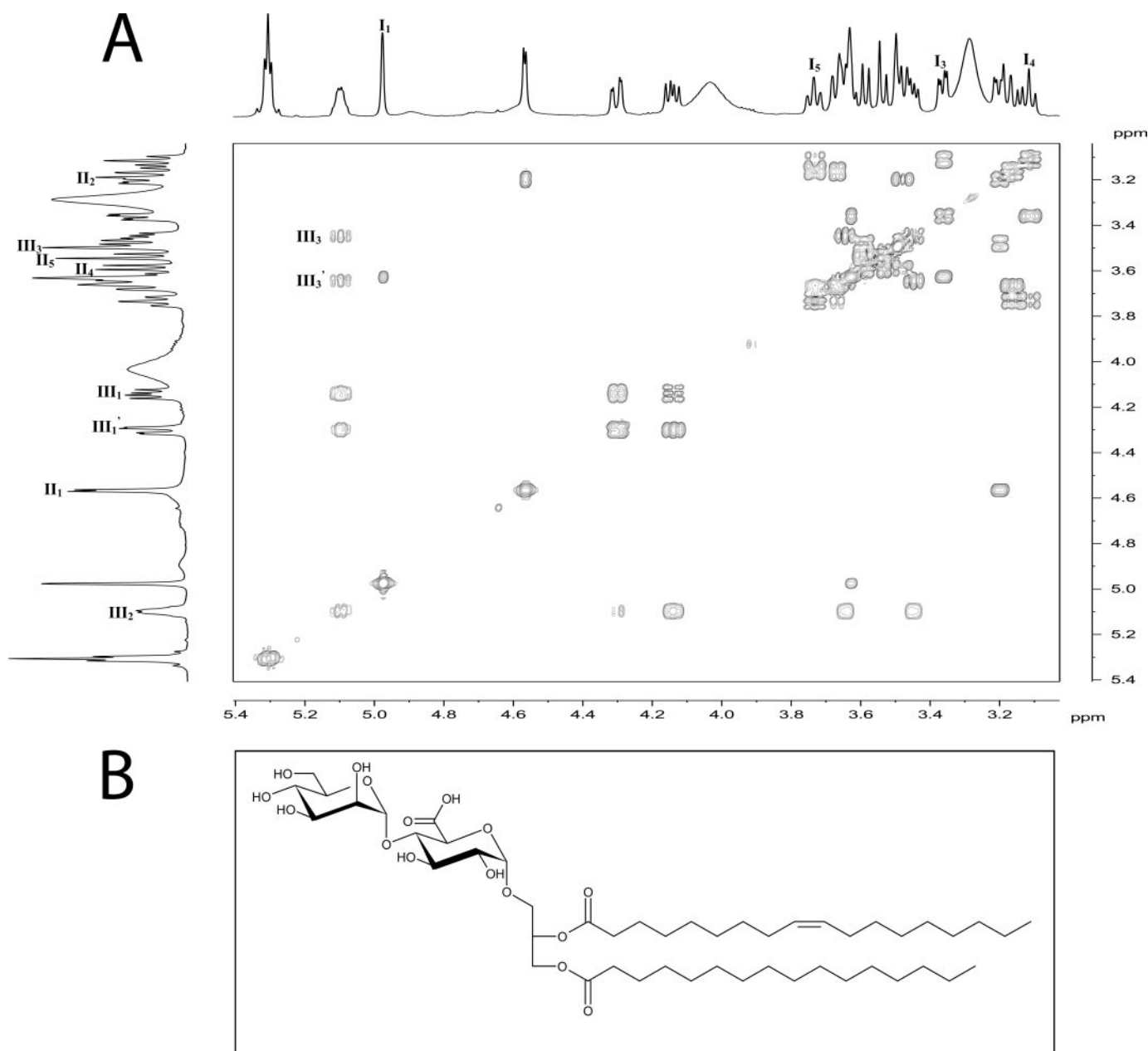


FIGURE 3. **Structural characterization of Gl-X.** A, two-dimensional ^1H - ^1H COSY NMR spectra of Gl-X recorded in d_6 - Me_2SO at 300 K. Glycosyl residues are labeled as *I* and *II*, glycerol is labeled as *III*, and their protons are labeled with *Arabic numerals*. B, chemical structure of Gl-X revealing ManGlcAGroAc₂.

In Vitro Analysis of Mannosyltransferase Activity—In order to confirm the mannosyltransferase activity and acceptor specificity of both Cg-PimB and Mt-PimB, we prepared membrane fractions from wild type *C. glutamicum*, the 13032::pimB mutant, and transformants of the latter bearing pEKEx3-Cg-pimB and pEKEx3-Mt-pimB. Analysis of radiolabeled mannosyl lipids, formed after introduction of GDP-[^{14}C]mannose by two-dimensional TLC (Fig. 2, E–H), revealed a clear difference between the profiles derived from the wild type strain and the 13032::pimB mutant. The upper spot of the dominant pair of glycolipids, corresponding to ManGlcAGroAc₂, is clearly absent in the mutant profile. Complementation with Cg-pimB in *trans*, as expected, restored ManGlcAGroAc₂ biosynthesis, and, consistent with our extracted lipid profiles, complementation with Mt-pimB was also achieved. In all of the profiles, the

second spot corresponding to Ac₁PIM₂ was evident, the apparent increase in its abundance in the 13032::pimB mutant profile being due to the absence of ManGlcAGroAc₂ when equal radioactivity was loaded on the plates. The identities of these two lipids were confirmed by staining of the same TLC plates with the Dittmer-Lester lipid phosphate reagent (data not shown).

Chemical Analysis of *C. glutamicum* Lipoglycans—We examined extracts of wild type *C. glutamicum* and the *C. glutamicum* 13032::pimB disruption mutant for lipoglycans by SDS-PAGE followed by staining for carbohydrates with either silver nitrate or Pro-Q Emerald stain for glycoconjugates. Extracts of wild type *C. glutamicum* contained two closely migrating lipoglycans (Fig. 5). Interestingly, the lower molecular weight lipoglycan was significantly reduced in the *C. glutamicum*

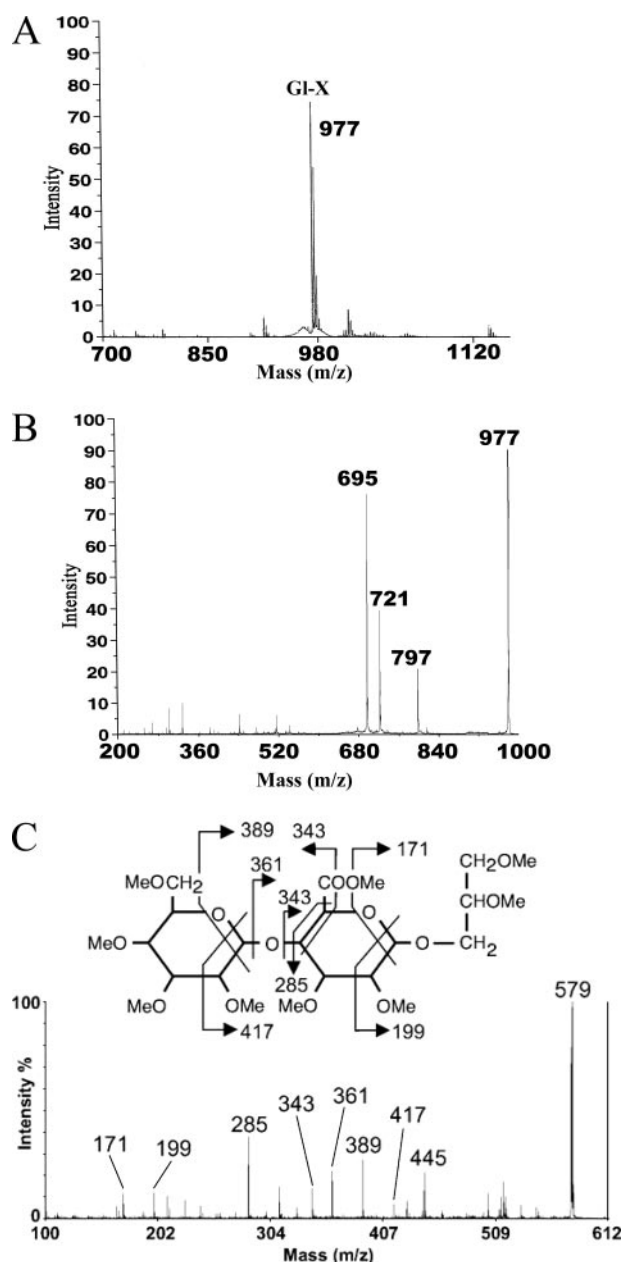


FIGURE 4. MALDI-TOF-MS analyses of GI-X. A, positive ion mode MALDI-TOF-MS analysis of GI-X. B, positive ion MALDI-TOF CID-MS/MS spectrum of the cationized sodiated precursor ion ($M - H + 2Na$)⁺ of GI-X at m/z 977 with ions at m/z 721 and 695 corresponding to the loss of C_{16} and $C_{18:1}$ fatty acids, respectively. C, MALDI-TOF/TOF-MS analysis of methylated glycan obtained from GI-X. The molecular ion at m/z 579 ($M + Na$)⁺ was selected for CID-MS/MS. Informative fragment ions are shown schematically (inset). The fragment ion at m/z 445 results from the glycerol moiety via cleavage on the reducing side of the glycosidic bond with concomitant loss of CH_3OH .

TABLE 3

¹H and ¹³C NMR assignment of key resonances of GI-X

| Residue | Chemical shifts | | | | | |
|-----------------------|-------------------|--------------|-------------------|--------------|-------------------|-------------------|
| | H-1 C-1 | H-2 C-2 | H-3 C-3 | H-4 C-4 | H-5/(H-5') C-5 | H-6/H-6' C-6 |
| | ppm | | | | | |
| t- α -Manp (I) | 4.98 100.3 | 3.64 70.4 | 3.38 71.0 | 3.13 68.3 | 3.74 73.1 | 3.67/3.17 62.1 |
| α -GlcA (II) | 4.57 99.0 | 3.19 71.7 | 3.48 72.8 | 3.59 78.6 | 3.53 74.1 | |
| Glycerol (III) | 4.15/4.31 62.2 | 5.09 69.4 | 3.45/3.65 64.8 | | | 171.6 |

13032::pimB mutant (Fig. 5). A two-step purification protocol was performed to fractionate the lipoglycans from wild type *C. glutamicum* and the *C. glutamicum* 13032::pimB mutant, and fractions containing the lipoglycans were monitored by SDS-PAGE stained with either silver nitrate or Pro-Q Emerald staining.

The larger lipoglycan from wild type *C. glutamicum* exhibited the basic components of a structure related to mycobacterial LAM and is, henceforth, termed Cg-LAM. GC analysis of the total acid-hydrolyzed Cg-LAM identified arabinose, mannose, and inositol in a ratio of 19:60:1. Per-*O*-methylation analysis of Cg-LAM indicated the presence of t-Araf, t-Manp, 2-Manp, 6-Manp, and 2,6-Manp (Fig. 6A). Accordingly, the ¹H-¹³C HMQC NMR anomeric region (Fig. 7, A and B) exhibited a pattern of resonances that could be attributed, based on our previous studies with mycobacterial LAMs and LAM-related structures, to these different units (45). Indeed, correlations at δ_{H1C1} 5.20/112.2 (I₁) and 5.13/112.0 (II₁) were attributed to two t-Araf units; 5.06/105.2 (III₁) to t-Manp units; 5.12/101.4 (IV₁), 5.07/101.7 (V₁), and 5.04/101.9 (VI₁) to 2,6-Manp units; 5.06/105.2 (VII₁) to 6-Manp units; and 5.00/104.9 (VIII₁) to 2-Manp units. Altogether, these data indicate that Cg-LAM is composed of a PI anchor linked to an α (1→6)Manp backbone substituted at most of the O-2 positions by t-Araf, t-Manp, t-Araf(1→2)-Manp, and t-Manp(1→2)-Manp units (Fig. 7C).

In a similar manner, GC analysis of the smaller lipoglycan (Cg-LM) from wild type *C. glutamicum* contained solely mannose and no trace of inositol. Per-*O*-methylation analysis of the smaller lipoglycan (Cg-LM) indicated the presence of t-Manp, 2-Manp, 6-Manp, and 2,6-Manp (Fig. 6B). Accordingly, the ¹H-¹³C HMQC NMR anomeric region (Fig. 8, A and B) of Cg-LM exhibited correlations at δ_{H1C1} 5.16/101.4 (I₁) and 5.08/105.4 (II₁) that were attributed to 2,6-Manp and t-Manp units, respectively. Resonances at δ_{H1} 4.96, 4.95, and 4.94 (IV_{1a,b,c}) that correlated on the two-dimensional ¹H-¹H HOHAHA (Fig. 8C) of the Cg-LM spectrum with δ_{H2} 4.04 typified the 6-Manp units usually found in the mannan core of mycobacterial lipoglycans and spin system III₁ ($\delta_{H1/H2}$ 5.03/4.11) characterized 2-Manp units. The ¹H-¹H HOHAHA (Fig. 8C) spectrum also showed two spin systems with weaker intensity. Resonances at δ 5.25 (Vb₂) and 5.29 (Va₂) exhibited correlations with proton resonances at δ 4.22 (Vb₁), 4.11 (Vb₁), 3.93 (Vb_{3/3'}) and 4.16 (Vb₁), 4.01 (Vb₁), 3.88 (Vb_{3/3'}), respectively. These spin systems were attributed to diacylated glycerol units characterized by deshielded H-2 resonances (5.25 and 5.29 ppm). The NMR data also confirm that Cg-LM also appears to lack inositol and is composed of a diacylglycerol unit linked to an α (1→6)Manp

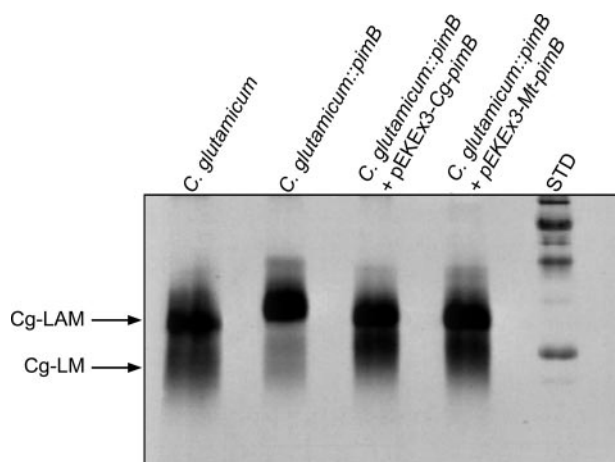


FIGURE 5. Lipoglycan profiles of wild type *C. glutamicum*, *C. glutamicum* 13032::pimB, and *C. glutamicum* 13032::pimB complemented with either Cg-pimB or Mt-pimB. Lipoglycans were analyzed using SDS-PAGE and visualized using the Pro-Q emerald glycoprotein stain (Invitrogen) specific for carbohydrates. The STD lane contains CandyCane glycoprotein molecular weight standards (Invitrogen). The four major bands represent glycoproteins of 180, 82, 42, and 18 kDa, respectively.

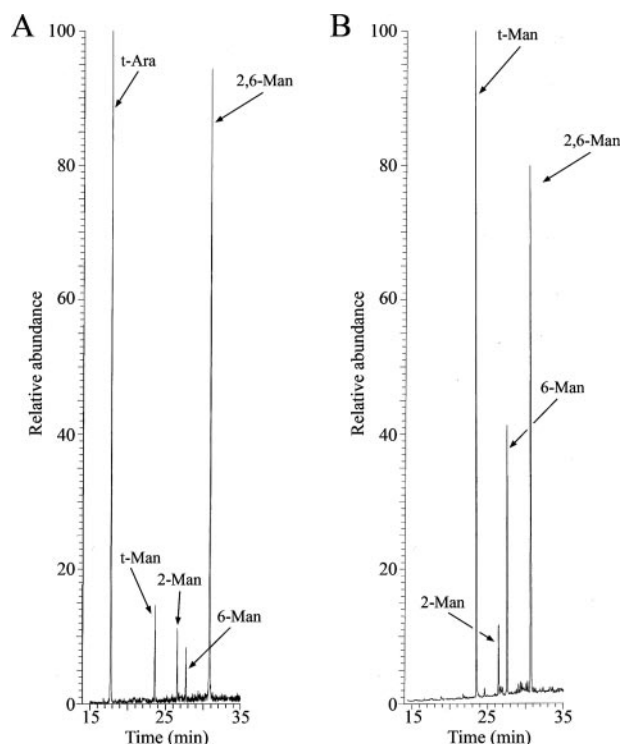


FIGURE 6. Glycosidic linkage analysis of lipoglycans from *C. glutamicum*. Per-*O*-methylated samples were hydrolyzed and per-*O*-acetylated. The resulting alditol acetates from Cg-LAM (A) and Cg-LM (B) were analyzed by GC and gas chromatography/mass spectrometry (GC/MS) (37).

backbone substituted at most of the O-2 positions by t-Manp and t-Manp(1→2)-Manp units (Fig. 8D).

Interestingly, in comparison with wild type *C. glutamicum*, the *C. glutamicum* 13032::pimB disruption mutant and analysis by SDS-PAGE using Pro-Q Emerald stain for glycoconjugates revealed that the upper lipoglycan appears unaffected (Fig. 5). This was confirmed by glycosyl compositional analysis and per-*O*-methylation analysis of Cg-pimB LAM (data not shown). However, the smaller lipoglycan, Cg-pimB-LM, was now barely

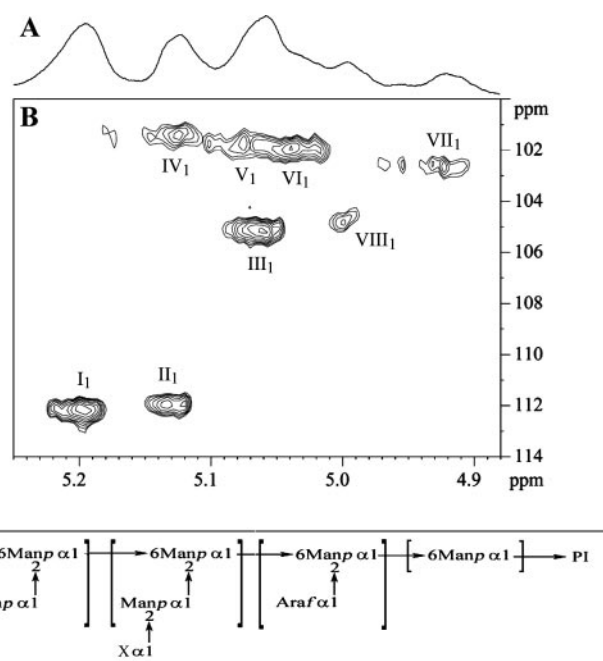


FIGURE 7. Structural characterization of wild type Cg-LAM. One-dimensional ^1H (A) and two-dimensional ^1H - ^{13}C HMQC (B) NMR spectra of Cg-LAM in D_2O at 313 K. Expanded regions (δ ^1H : 4.88–5.25) (A) and (δ ^1H : 4.88–5.25, δ ^{13}C : 100–114) (B) are shown. Glycosyl residues are labeled in Roman numerals, and their carbons and protons are labeled in Arabic numerals. I, II, t- α -Araf; III, t- α -Manp; IV, V, VI, 2,6- α -Manp; VII, 6- α -Manp; VIII, 2- α -Manp. C, structural representation of Cg-LAM. Cg-LAM contains an $\alpha(1\rightarrow6)$ -Manp backbone almost completely substituted by t-Araf, t-Manp, t-Manp(1→2)-Manp, and t-Araf(1→2)-Manp units. X, either a t-Araf or a t-Manp unit.

detectable (Fig. 5). Glycosyl compositional analysis of the residual Cg-pimB-LM now revealed the presence of both mannose and inositol (47:1), and per-*O*-methylation analysis indicated the presence of t-Manp, 2-Manp, 6-Manp, and 2,6-Manp (data not shown). Furthermore, ^1H NMR spectra exhibited an anomeric region with the typical resonances corresponding to these different units (data not shown). The pattern was simpler than that observed for the wild type Cg-LM and corresponded to the profile typically observed for mycobacterial PI-based LM. Integration of the resonances indicated a mannan core with a reduced branching degree as compared with the wild type Cg-LM.

In summary, these results suggest that Cg-LM is most likely two components, a dominant Cg-LM based on the ManGlcA-GroAc₂ and a minor component akin to the characteristic mycobacterial PI-based LM.

DISCUSSION

Along with the genus *Mycobacterium*, species of *Corynebacterium* belong to a suprageneric actinomycete taxon termed *Corynebacterianeae*, which also includes *Rhodococcus*, *Nocardia*, and other closely related genera. In this study, we sought to establish the role of Cg-PimB and Mt-PimB and whether *C. glutamicum* possesses both PIMs and lipoglycans reminiscent of *M. tuberculosis* products, suggesting conserved biosynthetic machineries within these two bacteria. In *M. tuberculosis*, Mt-pimB (Rv0557) was shown earlier to encode an α -D-mannose- $\alpha(1\rightarrow6)$ -phosphatidyl-*myo*-inositol-monomannoside mannosyltransferase and to be involved in the formation of Ac₁PIM₂

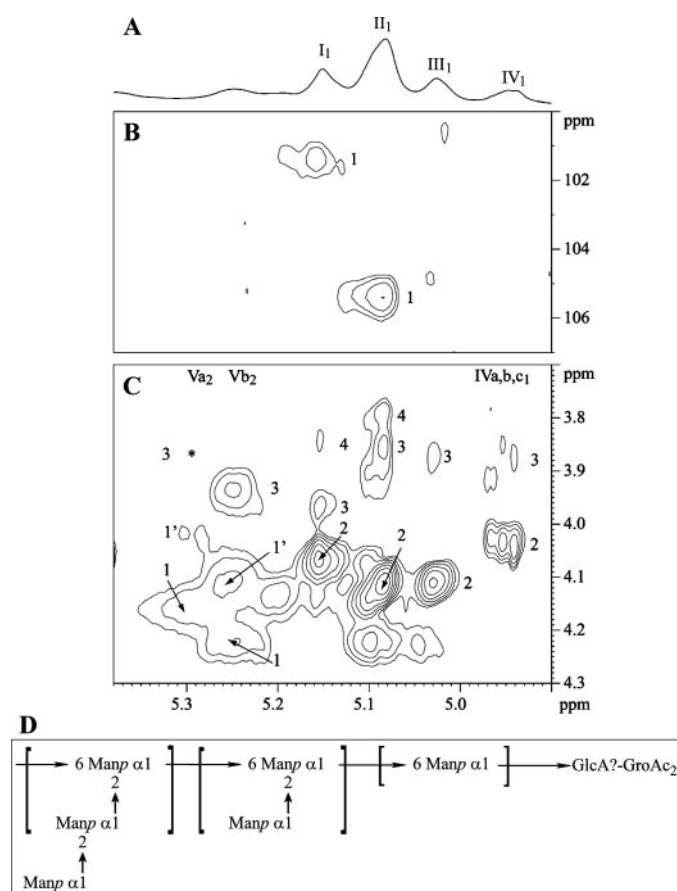


FIGURE 8. Structural characterization of Cg-LM. One-dimensional ^1H (A), two-dimensional ^1H - ^{13}C HMQC (B), and two-dimensional ^1H - ^1H HOHAHA τ_m 110-ms NMR spectra of CgLM in D_2O at 313 K. Expanded regions ($\delta^1\text{H}$: 4.90–5.38 (A); $\delta^1\text{H}$: 4.90–5.38, $\delta^{13}\text{C}$: 100–107 (B); and $\delta^1\text{H}$: 4.90–5.38, $\delta^1\text{H}$: 3.70–4.30 (C)) are shown. Glycosyl residues are labeled in *Roman numerals*, and their carbons and protons are labeled in *Arabic numerals*. I, 2,6- α -Manp; II, t- α -Manp; III, 2- α -Manp; IV, 6- α -Manp; V, Gro. D, structural representation of Cg-LM. Cg-LM contains an $\alpha(1\rightarrow6)$ -Manp backbone partially substituted at O-2 by t-Manp, t-Manp(1 \rightarrow 2)-Manp units.

from GDP-mannose and Ac_1PIM_1 (19). In this study, we attempted to disrupt *Cg-pimB* and examine the consequences of PIM and LAM biosynthesis in *C. glutamicum*.

To our surprise and unrelated to PIMs, the *C. glutamicum* 13032::*pimB* disruption mutant was found to possess major differences in cell wall lipids and lipoglycans in comparison with the parental *C. glutamicum* strain. A novel glycolipid, which we initially termed GI-X and subsequently characterized as 1,2-di- $\text{O-C}_{16}/\text{C}_{18:1}$ -(α -D-mannopyranosyl)-(1 \rightarrow 4)-(α -D-glucopyranosyluronic acid)-(1 \rightarrow 3)-glycerol (ManGlcAGroAc₂), from wild type *C. glutamicum* was absent in the *C. glutamicum* 13032::*pimB* disruption mutant. Strikingly, the biosynthesis of this novel lipid, ManGlcAGroAc₂, was restored when complemented with either *Cg-PimB* or *Mt-PimB*.

These results raised several interesting questions and possibilities concerning the biochemical role and function of *Cg-PimB* and *Mt-PimB*, the immediate question being whether *Cg-PimB* represents a GDP-mannose-dependent α -mannosyltransferase or adds glucopyranosyluronic acid to a diacylated glycerol precursor. During our purification process of polar lipids, we isolated and characterized in the *C. glutamicum* 13032::*pimB* disruption mutant a second phosphorus-free gly-

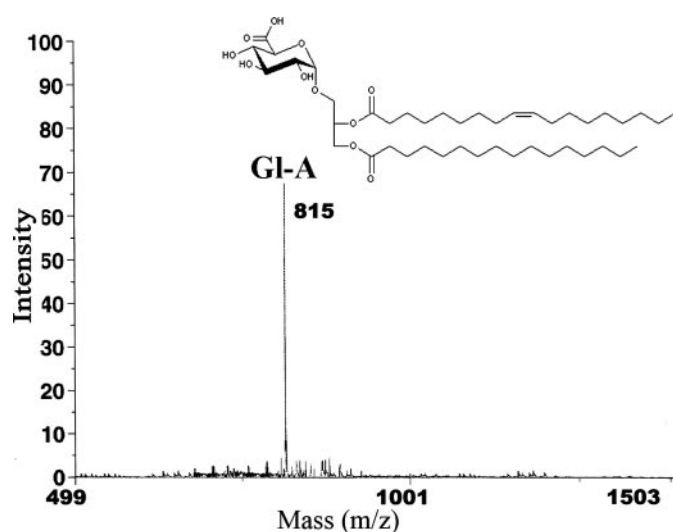


FIGURE 9. Positive ion mode MALDI-MS analysis of GI-A isolated from the *C. glutamicum* 13032::*pimB* disruption mutant. Spectra from 2500–5000 laser shots were summed to obtain the final spectrum. Typically, 0.3 μl of GI-A (at 10 mg/ml in $\text{CHCl}_3/\text{CH}_3\text{OH}$, 1:1, v/v) and 0.3 μl of the matrix solution (2,5-dihydrobenzoic acid at ~ 10 mg/ml in $\text{C}_2\text{H}_5\text{OH}/\text{H}_2\text{O}$, 1:1, v/v) were deposited on the target, revealing GI-A ($\text{M} - \text{H} + 2\text{Na}$) $^+$ at m/z 815.

colipid, which we termed GI-A (Fig. 2). GI-A was subsequently analyzed both in negative and positive mode MALDI-MS. Spectra were only obtained in positive mode, revealing a molecular ion at m/z 815 ($\text{M} - \text{H} + 2\text{Na}$) $^+$ (Fig. 9), which is in agreement with previous reports of a 1,2-di- O -acyl-(α -D-glucopyranosyluronic acid)-(1 \rightarrow 3)-glycerol, which would represent the precursor of ManGlcAGroAc₂ as GlcAGroAc₂ (46). This would suggest that *PimB* represents a *bona fide* α -mannosyltransferase, which we have now reassigned as an α -mannosylglucopyranosyluronic acid-transferase A (*MgtA*), to a diacylated glucuronosyl glycerol involved in ManGlcAGroAc₂ biosynthesis, since the synthesis of GlcAGroAc₂ remained unaffected in the *C. glutamicum* 13032::*pimB* disruption mutant. This assignment is wholly compatible with our *in vitro* mannosylation data. Interestingly, we observed no consistent accumulation of GI-A as might be expected, although the amounts of the lipid were increased in some cultures. Presumably, the regulation of this pathway is complex and will require careful study.

Glycosylated diacylglycerols are commonly found in Gram-positive bacteria as well as in higher plants. It was previously established that these glycosylated diacylglycerols function as precursors/anchors for hyperglycosylated variants, such as the lipomannans, as found in the case of dimannosyl diacylglycerols in *Micrococcus* and lipoteichoic acids (47–49). Moreover, related di- and monoacylglycerols containing glucuronosyl residues have been well reported in *Pseudomonas* spp. (50–52), *Bacillus cereus* T (53), and halotolerant bacteria (54–57). In relation to *Mycobacterium*, the data are sparse in regards to the presence of glycosyl diacylglycerols, except for a few limited cases, such as a diglucosyl diacylglycerol (58). The presence of the uronic acid residue in ManGlcAGroAc₂ is interesting due to its rarity with regard to the published literature, especially with reference to *Mycobacterium* spp. In mycobacteria to date, a glucuronosyl diacylglycerol in *Mycobacterium smegmatis* (46), uronosyl-containing glycopeptidolipid in *Mycobacterium*

avium (59–61), and a uronosyl-containing polar glycopeptidolipid in *Mycobacterium habana* (62) have been reported. This is the first description of its kind in *Corynebacteriaceae* of a mannosylated variant of glucuronosyl diacylglycerol.

Our results also suggest that ManGlcAGroAc₂ also participates in the biosynthesis of a novel Cg-LM-like molecule. The above notion is based on two observations. First, when ManGlcAGroAc₂ is not synthesized in the *C. glutamicum* 13032::pimB mutant, the production of Cg-LM is greatly reduced, but when complemented with either Cg-pimB, Cg-LM biosynthesis is restored (Fig. 5). Second, glycosyl compositional analysis of the residual Cg-pimB-LM revealed the presence of both mannose and inositol. Per-O-methylation analysis indicated the presence of t-Manp, 2,6-Manp, and 6-Manp. The pattern was simpler than that observed for the wild type Cg-LM and corresponded to the profile typically observed for mycobacterial PI-based LM. In summary, these results suggest that Cg-LM is most likely two components, a dominant Cg-LM based on the ManGlcAGroAc₂ and a minor component akin to the characteristic mycobacterial PI-based LM.

Although Cg-LM and Cg-LAM are consistent in belonging to the LM/LAM archetype, these lipoglycans are notably distinct from mycobacterial LAMs. In addition, given the potent immunomodulatory effects of PIMs/LM/LAM from *M. tuberculosis*, the possibility that similar products to Gl-X, Gl-A, and related lipoglycans could exist in *M. tuberculosis* is intriguing. We are currently developing methods to fractionate polar lipids and lipoglycans from *M. tuberculosis* in a search for such novel glycolipids. Linked to this is the question of the role of Mt-PimB. Our results clearly show that Cg-pimB plays no crucial role in PIM biosynthesis in *C. glutamicum*. However, since relaxed substrate specificities in microbial glycosyltransferases have been recorded on heterospecific expression (63), we must not overinterpret the ability of Mt-pimB to complement the lesion in ManGlcAGroAc₂ biosynthesis in our *C. glutamicum* 13032::pimB mutant. The possibility remains that the *M. tuberculosis* PimB does contribute to the biosynthesis of PIMs but merely has relaxed acceptor specificity and is able to utilize GlcAGroAc₂. The clear definition of the substrate specificities of these enzymes will require their purification to homogeneity, and toward this we have attempted to construct a number of fusion proteins to afford a facile purification protocol but have yet to produce soluble recombinant protein. A protocol yielding active soluble protein is now being sought to address this point.

Acknowledgment—We thank Nick May for MS analyses.

REFERENCES

- Bloom, B. R., and Murray, C. J. (1992) *Science* **257**, 1055–1064
- Coyle, M. B., and Lipsky, B. A. (1990) *Clin. Microbiol. Rev.* **3**, 227–246
- Funke, G., von Graevenitz, A., Clarridge, J. E., III, and Bernard, K. A. (1997) *Clin. Microbiol. Rev.* **10**, 125–159
- Sahm, H., Eggeling, L., and de Graaf, A. A. (2000) *Biol. Chem.* **381**, 899–910
- Stackebrandt, E., Rainey, F. A., and Ward-Rainey, N. L. (1997) *Int. J. Syst. Bacteriol.* **47**, 479–491
- Brennan, P. J. (2003) *Tuberculosis (Edinb.)* **83**, 91–97
- McNeil, M., Daffe, M., and Brennan, P. J. (1990) *J. Biol. Chem.* **265**, 18200–18206
- Besra, G. S., Khoo, K. H., McNeil, M. R., Dell, A., Morris, H. R., and Brennan, P. J. (1995) *Biochemistry* **34**, 4257–4266
- Daffe, M., Brennan, P. J., and McNeil, M. (1990) *J. Biol. Chem.* **265**, 6734–6743
- McNeil, M., Daffe, M., and Brennan, P. J. (1991) *J. Biol. Chem.* **266**, 13217–13223
- Dover, L. G., Cerdeno-Tarraga, A. M., Pallen, M. J., Parkhill, J., and Besra, G. S. (2004) *FEMS Microbiol. Rev.* **28**, 225–250
- Brennan, P. J., and Nikaido, H. (1995) *Annu. Rev. Biochem.* **64**, 29–63
- Dmitriev, B. A., Ehlers, S., Rietschel, E. T., and Brennan, P. J. (2000) *Int. J. Med. Microbiol.* **290**, 251–258
- Morita, Y. S., Patterson, J. H., Billman-Jacobe, H., and McConville, M. J. (2004) *Biochem. J.* **378**, 589–597
- Besra, G. S., Morehouse, C. B., Rittner, C. M., Waechter, C. J., and Brennan, P. J. (1997) *J. Biol. Chem.* **272**, 18460–18466
- Brennan, P., and Ballou, C. E. (1967) *J. Biol. Chem.* **242**, 3046–3056
- Brennan, P., and Ballou, C. E. (1968) *J. Biol. Chem.* **243**, 2975–2984
- Hill, D. L., and Ballou, C. E. (1966) *J. Biol. Chem.* **241**, 895–902
- Schaeffer, M. L., Khoo, K. H., Besra, G. S., Chatterjee, D., Brennan, P. J., Belisle, J. T., and Inamine, J. M. (1999) *J. Biol. Chem.* **274**, 31625–31631
- Kremer, L., Gurucha, S. S., Bifani, P., Hitchen, P. G., Baulard, A., Morris, H. R., Dell, A., Brennan, P. J., and Besra, G. S. (2002) *Biochem. J.* **363**, 437–447
- Kordulakova, J., Gilleron, M., Mikusova, K., Puzo, G., Brennan, P. J., Gicquel, B., and Jackson, M. (2002) *J. Biol. Chem.* **277**, 31335–31344
- Gurucha, S. S., Baulard, A. R., Kremer, L., Loch, C., Moody, D. B., Muhlecker, W., Costello, C. E., Crick, D. C., Brennan, P. J., and Besra, G. S. (2002) *Biochem. J.* **365**, 441–450
- Morita, Y. S., Sena, C. B., Waller, R. F., Kurokawa, K., Sernee, M. F., Nakatani, F., Haite, R. E., Billman-Jacobe, H., McConville, M. J., Maeda, Y., and Kinoshita, T. (2006) *J. Biol. Chem.* **281**, 25143–25155
- Kaur, D., Berg, S., Dinadayala, P., Gicquel, B., Chatterjee, D., McNeil, M. R., Vissa, V. D., Crick, D. C., Jackson, M., and Brennan, P. J. (2006) *Proc. Natl. Acad. Sci. U. S. A.* **103**, 13664–13669
- Dinadayala, P., Kaur, D., Berg, S., Amin, A. G., Vissa, V. D., Chatterjee, D., Brennan, P. J., and Crick, D. C. (2006) *J. Biol. Chem.* **281**, 20027–20035
- Grant, S. G., Jesse, J., Bloom, F. R., and Hanahan, D. (1990) *Proc. Natl. Acad. Sci. U. S. A.* **87**, 4645–4649
- Schafer, A., Tauch, A., Jager, W., Kalinowski, J., Thierbach, G., and Puhler, A. (1994) *Gene (Amst.)* **145**, 69–73
- Eggeling, L., and Reyes, O. (2005) *Handbook of Corynebacterium Glutamicum* (Eggeling, L., and Bott, M., eds) pp. 535–566, CRC Press, Inc., Boca Raton, FL
- Dobson, G., Minnikin, D. E., Minnikin, S. M., Parlett, M., Goodfellow, M., Ridell, M., and Magnusson, M. (1985) in *Chemical Methods in Bacterial Systematics* (Goodfellow, M., and Minnikin, D. E., eds) pp. 237–265, Academic Press, Inc., London
- Ryu, E. K., and MacCoss, M. (1979) *J. Lipid Res.* **20**, 561–563
- Nigou, J., Gilleron, M., Cahuzac, B., Bounery, J. D., Herold, M., Thurnher, M., and Puzo, G. (1997) *J. Biol. Chem.* **272**, 23094–23103
- Ludwiczak, P., Gilleron, M., Bordat, Y., Martin, C., Gicquel, B., and Puzo, G. (2002) *Microbiology* **148**, 3029–3037
- Leopold, K., and Fischer, W. (1993) *Anal. Biochem.* **208**, 57–64
- Hunter, S. W., Gaylord, H., and Brennan, P. J. (1986) *J. Biol. Chem.* **261**, 12345–12351
- Nigou, J., Vercellone, A., and Puzo, G. (2000) *J. Mol. Biol.* **299**, 1353–1362
- Ciucanu, I., and Kerek, F. (1984) *Carbohydr. Res.* **131**, 209–217
- Alderwick, L. J., Radmacher, E., Seidel, M., Gande, R., Hitchen, P. G., Morris, H. R., Dell, A., Sahm, H., Eggeling, L., and Besra, G. S. (2005) *J. Biol. Chem.* **280**, 32362–32371
- Gilleron, M., Quesniaux, V. F., and Puzo, G. (2003) *J. Biol. Chem.* **278**, 29880–29889
- Gilleron, M., Nigou, J., Cahuzac, B., and Puzo, G. (1999) *J. Mol. Biol.* **285**, 2147–2160
- Gilleron, M., Bala, L., Brando, T., Vercellone, A., and Puzo, G. (2000)

Identification of a Novel Mannosylated Glycolipid

- J. Biol. Chem.* **275**, 677–684
41. Sassetti, C. M., Boyd, D. H., and Rubin, E. J. (2003) *Mol. Microbiol.* **48**, 77–84
 42. Nakamura, Y., Nishio, Y., Ikeo, K., and Gojobori, T. (2003) *Gene (Amst.)* **317**, 149–155
 43. Gibson, K. J., Eggeling, L., Maughan, W. N., Krumbach, K., Gurcha, S. S., Nigou, J., Puzo, G., Sahm, H., and Besra, G. S. (2003) *J. Biol. Chem.* **278**, 40842–40850
 44. Allard, S. T., Giraud, M. F., and Naismith, J. H. (2001) *Cell Mol. Life Sci.* **58**, 1650–1665
 45. Gibson, K. J., Gilleron, M., Constant, P., Puzo, G., Nigou, J., and Besra, G. S. (2003) *Microbiology* **149**, 1437–1445
 46. Wolucka, B. A., McNeil, M. R., Kalbe, L., Cocito, C., and Brennan, P. J. (1993) *Biochim. Biophys. Acta* **1170**, 131–136
 47. Pieringer, R. A. (1989) in *Microbial Lipids* (Ratledge, C., and Wilkinson, S. G., eds) Vol. 2, pp. 51–114, Academic Press, Inc., London
 48. Pakkiri, L. S., and Waechter, C. J. (2005) *Glycobiology* **15**, 291–302
 49. Pakkiri, L. S., Wolucka, B. A., Lubert, E. J., and Waechter, C. J. (2004) *Glycobiology* **14**, 73–81
 50. Wilkinson, S. G. (1968) *Biochim. Biophys. Acta* **164**, 148–156
 51. Wilkinson, S. G. (1969) *Biochim. Biophys. Acta* **187**, 492–500
 52. Wilkinson, S. G. (1968) *Biochim. Biophys. Acta* **152**, 227–229
 53. Minnikin, D. E., Abdolrahimzadeh, H., and Baddiley, J. (1971) *Biochim. Biophys. Acta* **249**, 651–655
 54. Peleg, E., and Tietz, A. (1971) *FEBS Lett.* **15**, 309–312
 55. Stern, N., and Tietz, A. (1973) *Biochim. Biophys. Acta* **296**, 136–144
 56. Stern, N., and Tietz, A. (1973) *Biochim. Biophys. Acta* **296**, 130–135
 57. Stern, N., and Tietz, A. (1971) *FEBS Lett.* **19**, 217–220
 58. Hunter, S. W., McNeil, M. R., and Brennan, P. J. (1986) *J. Bacteriol.* **168**, 917–922
 59. Chatterjee, D., Aspinall, G. O., and Brennan, P. J. (1987) *J. Biol. Chem.* **262**, 3528–3533
 60. Chatterjee, D., Bozic, C., Aspinall, G. O., and Brennan, P. J. (1988) *J. Biol. Chem.* **263**, 4092–4097
 61. McNeil, M., Chatterjee, D., Hunter, S. W., and Brennan, P. J. (1989) *Methods Enzymol.* **179**, 215–242
 62. Khoo, K. H., Chatterjee, D., Dell, A., Morris, H. R., Brennan, P. J., and Draper, P. (1996) *J. Biol. Chem.* **271**, 12333–12342
 63. Luneberg, E., Zetzmann, N., Alber, D., Knirel, Y. A., Kooistra, O., Zahring, U., and Frosch, M. (2000) *Int. J. Med. Microbiol.* **290**, 37–49

Inactivation of *Corynebacterium glutamicum* NCgl0452 and the Role of MgtA in the Biosynthesis of a Novel Mannosylated Glycolipid Involved in Lipomannan Biosynthesis

Raju V. V. Tatituri, Petr A. Illarionov, Lynn G. Dover, Jerome Nigou, Martine Gilleron, Paul Hitchen, Karin Krumbach, Howard R. Morris, Neil Spencer, Anne Dell, Lothar Eggeling and Gurdyal S. Besra

J. Biol. Chem. 2007, 282:4561-4572.

doi: 10.1074/jbc.M608695200 originally published online December 19, 2006

Access the most updated version of this article at doi: [10.1074/jbc.M608695200](https://doi.org/10.1074/jbc.M608695200)

Alerts:

- [When this article is cited](#)
- [When a correction for this article is posted](#)

[Click here](#) to choose from all of JBC's e-mail alerts

This article cites 59 references, 30 of which can be accessed free at <http://www.jbc.org/content/282/7/4561.full.html#ref-list-1>